Available online at www.sciencedirect.com

SciVerse ScienceDirect

Journal of Nutritional Biochemistry 23 (2012) 349–360

Journal of Nutritional Biochemistry

Cyanidin 3-glucoside attenuates obesity-associated insulin resistance and hepatic steatosis in high-fat diet-fed and *db*/*db* mice via the transcription factor FoxO1☆

Honghui Guo[a,b], Min Xia[a,*], Tangbin Zou[a], Wenhua Ling[a,*], Ruimin Zhong[b], Weiguo Zhang[b]

[a]Guangdong Provincial Key Laboratory of Food, Department of Nutrition, School of Public Health, Sun Yat-Sen University (Northern Campus), Guangzhou 510080, China
[b]Department of Food Science, Yingdong College of Bioengineering, Shaoguan University, Shaoguan 512005, China

Received 2 August 2010; received in revised form 7 December 2010; accepted 7 December 2010

Abstract

Obesity is a major risk factor for the development of type 2 diabetes, and both conditions are now recognized to possess significant inflammatory components underlying their pathophysiologies. Here, we hypothesized that cyanidin 3-glucoside (C3G), a typical anthocyanin reported to possess potent anti-inflammatory properties, would ameliorate obesity-associated inflammation and metabolic disorders, such as insulin resistance and hepatic steatosis in mouse models of diabesity. Male C57BL/6J obese mice fed a high-fat diet for 12 weeks and genetically diabetic *db*/*db* mice at an age of 6 weeks received dietary C3G supplementation (0.2%) for 5 weeks. We found that dietary C3G lowered fasting glucose levels and markedly improved the insulin sensitivity in both high-fat diet fed and *db*/*db* mice as compared with unsupplemented controls. White adipose tissue messenger RNA levels and serum concentrations of inflammatory cytokines (tumor necrosis factor-α, interleukin-6, and monocyte chemoattractant protein-1) were reduced by C3G, as did macrophage infiltration in adipose tissue. Concomitantly, hepatic triglyceride content and steatosis were alleviated by C3G. Moreover, C3G treatment decreased c-Jun N-terminal kinase activation and promoted phosphorylation and nuclear exclusion of forkhead box O1 after refeeding. These findings clearly indicate that C3G has significant potency in antidiabetic effects by modulating the c-Jun N-terminal kinase/forkhead box O1 signaling pathway and the related inflammatory adipocytokines.

Keywords: Anthocyanin; c-Jun N-terminal kinase; Forkhead box O1; Inflammation; Insulin resistance; Hepatic steatosis

1. Introduction

Obesity-associated inflammation contributes to many clinically important complications, such as insulin resistance, type 2 diabetes, nonalcoholic fatty liver disease and cardiovascular disease [1]. Although the cause and the molecular participants in this process remain incompletely defined, adipose tissue plays a central role. Studies have shown that dysregulation of adipose tissue-derived free fatty acids and adipocytokines results in impaired insulin sensitivity of other tissues, including the liver, skeletal muscle, pancreatic islets (β cells) and central nervous system [2]. Among those so-called adipocytokines, tumor necrosis factor-α (TNF-α), interleukin-6 (IL-6) and monocyte chemoattractant protein-1 (MCP-1) are up-regulated in adipose tissue and plasma by obesity and in type 2 diabetes, whereas adiponectin is down-regulated [1]. Investigators also found that obese adipose tissue is characterized by macrophage infiltration [3], which serves as an important source of inflammation. It has been shown that TNF-α and IL-6 are key mediators of hepatic inflammation, liver cell death, fibrosis and liver regeneration after injury [4,5]. Moreover, decreased plasma adiponectin concentrations are closely associated with nonalcoholic hepatic steatosis in obese individuals [6], suggesting that metabolic dysregulation may be aggravated systemically by these adipose tissue-derived factors. Therefore, reducing obesity-induced inflammation by the modulation of adipocytokines secretion and actions may be a useful strategy for preventing obesity-associated metabolic pathologies.

In addition to inflammatory cytokines and intercellular signalling molecules, recent data have implicated several intracellular pathways that regulate the process of obesity-induced insulin resistance. Among them, forkhead box O1 (FoxO1) has been advanced as a major transcriptional mediator of insulin signaling in many cells, such as pancreatic β cell, adipocyte and hepatocyte [7–9]. FoxO1 transcriptional activity is positively regulated by stress-activated c-Jun N-terminal kinase (JNK) via promoting its import in the nucleus [10,11]. On the contrary, insulin/growth factor-activated protein kinase B (Akt) phosphorylates FoxO1 at three conserved Ser/Thr residues, leading to nuclear exclusion and the subsequent down-regulation of target genes expression [12]. Loss- or gain-of-function animal models of FoxO1 have clearly demonstrated that FoxO1 is a negative regulator of insulin sensitivity. For instance, transgenic mice expressing a constitutively active FoxO1 allele exhibited insulin resistance and hepatic steatosis [13], whereas antisense oligonucleotide-mediated target reduction of FoxO1 in the liver or adipose tissue

☆ This work was supported by the research grants from National Natural Science Foundation of China (30800913; 30700665; 30730079) and Natural Science Foundation of Guangdong Province China (8451200501000168).
* Corresponding author. Tel.: +86 20 87331597; fax: +86 20 87330446.
E-mail addresses: xiamin@mail.sysu.edu.cn (M. Xia), lingwh@mail.sysu.edu.cn (W. Ling).

0955-2863/$ - see front matter.
doi:10.1016/j.jnutbio.2010.12.013

improves glucose tolerance and peripheral insulin action in mice with diet-induced obesity [14,15]. Recently, Ito et al. [16] demonstrated that knockdown of FoxO1 by small-interfering RNA transfection inhibits TNF-α-induced expression of MCP-1 and IL-6 in 3T3-L1 adipocytes, indicating that FoxO1 regulation is also likely to be critical in the expression of inflammatory cytokines in adipose tissue.

In recent years, dietary strategies for alleviating the metabolic complications of obesity are being pursued as alternatives to pharmaceutical interventions. Anthocyanins are naturally occurring polyphenolic compounds in higher plants and widely distributed in fruits, vegetables and pigmented cereals, suggesting that we can ingest significant amounts of anthocyanins from plant-based daily diets [17]. Many studies have shown that anthocyanins not only impart color to plant foods but also exhibit pharmacological properties. We previously demonstrated that cyanidin 3-glucoside (C3G), which is the most widespread anthocyanin in nature [18], significantly suppressed inflammatory signaling pathway in CD40-induced human endothelial cells, as well as the lipopolysaccharide-induced THP-1 macrophages [19,20]. Our prior studies also showed that C3G exerts a protective role against H_2O_2- or TNF-α-induced insulin resistance in 3T3-L1 adipocytes [21]. Furthermore, recent studies from us and other laboratories have shown that dietary supplementation of plant extracts rich in C3G is associated with improved insulin sensitivity in both diet-induced and genetic animal models of insulin resistance [22–25]. The results of these studies suggest that anthocyanins may have important implications in preventing obesity and type 2 diabetes. What is not clear from these studies is whether this effect is due to only C3G, or whether other polyphenols in the extracts have similar effects. Moreover, the molecular action of anthocyanin responsible for the amelioration of inflammation and the enhancement of insulin sensitivity is not yet fully understood *in vivo*.

Considered together, the present study was designed to examine whether the administration of purified C3G can decrease adipose inflammation and hepatic steatosis and alleviate insulin resistance in high-fat diet (HFD)-fed and *db*/*db* mice, two widely used animal models of obesity and type 2 diabetes. Concerning the molecular action and mechanism, the JNK- and Akt-mediated FoxO1 phosphorylation and nuclear exclusion were also investigated.

2. Materials and methods

2.1. Materials

C3G (purity ≥98%) was provided by Polyphenol AS (Sandnes, Norway). Antibodies specific for Akt, phospho-Akt (Ser-473), FoxO1 and phospho-FoxO1 (Thr-24) were from Cell Signaling Technology (Danvers, MA, USA); anti-JNK1, anti-β-actin and horseradish peroxidase-conjugated secondary antibodies were from Santa Cruz Biotechnology (Santa Cruz, CA, USA). Short-acting human insulin was purchased from Novo Nordisk (Bagsvaerd, Denmark). All other chemicals, unless otherwise indicated, were purchased from Sigma-Aldrich (St. Louis, MO, USA).

2.2. Experimental animals

Five-week-old C57BL/6J, C57BL/Ks *db*/*db* and *db*/+ male mice were obtained from Model Animal Research Center of Nanjing University (Nanjing, China) and housed in a temperature- and humidity-controlled environment with a 12-h light/dark cycle. C57BL/6J mice were maintained on AIN-93G standard fat diet [26], or AIN-93G modified by the addition of hydrogenated coconut oil to provide 58% of calories from fat (HFD) or HFD diet with the addition of 0.2% C3G (HFD+C3G). The *db*/*db* and *db*/+ mice were fed a standard AIN93-G chow throughout the experiments. For the HFD model, C3G treatment began after 12 weeks on the high-calorie diet. For the *db*/*db* model, dietary C3G supplementation (0.2%) began at 6 weeks of age (*db*/*db* +C3G). In both models, mice received dietary C3G intervention for 5 weeks. Twelve mice were used in each treatment group. Food was changed at intervals of 3 days to prevent oxidation of fat or C3G. All animals were allowed free access to food and water. Body weight (BW) and food intake were measured weekly throughout the study. All protocols were conducted in accord with the protocols approved by the Animal Care and Use Committee of Sun Yat-Sen University.

At the end of the experiment period, six mice of each group mice were killed by exsanguination after starvation for 12 h (fasted) or after starvation for 12 h followed by the provision of high-sucrose/fat-free diet (in order to stimulate insulin secretion and synchronize the eating patterns of all animals) for 2 h (refed). Serum samples were collected and kept at −80°C prior to use. The liver, heart, kidneys and adipose tissue (subcutaneous and epididymal) were removed and weighed, and samples were stored in RNAlater (Ambion, Austin, TX, USA) for subsequent isolation of RNA and analysis of gene expression, or frozen in liquid nitrogen and stored at −80°C or in 10% buffered neutral formalin for histological evaluation.

2.3. Glucose and insulin tolerance tests

Two days before the termination of the experiment, six mice of each group were subjected to a glucose tolerance test or insulin tolerance test. Mice were fasted for 8 h, followed by injection with glucose (1.5 g/kg BW for the HFD model; 1.0 g/kg BW for the *db*/*db* model) or regular human insulin (0.75 U/kg BW for the HFD model; 1.5 U/kg BW for the *db*/*db* model) into the peritoneal cavity. Blood samples of conscious mice were drawn from the tail vein at 0, 30, 60, 90 and 120 min after glucose/insulin injection, and the plasma glucose was determined using a portable glucometer (Roche Diagnostics, Shanghai, China).

2.4. Serum and liver tissue analyses

Serum levels of insulin were quantified using commercial enzyme-linked immunosorbent assay (ELISA) kits according to the manufacturer's instructions (BioVendor Laboratories, Guangzhou, China). Insulin resistance was estimated by the homeostatic model assessment, using the HOMA2 Calculator software as described by Levy et al. [27]. Serum cytokines (adiponectin, TNF-α, MCP-1 and IL-6) were analyzed using ELISA kits from Millipore (Billerica, MA, USA). Alanine aminotransferase levels that were assayed were determined in fresh serum using a Biosystem automatic biochemistry analyzer (Madrid, Spain). Unless specially notified, the presented data were from mice in fasted state.

Samples from the liver of each mouse were homogenized, the total lipids of the liver homogenates were extracted with a mixture of chloroform and methanol according to the method of Folch et al. [28], and the amounts of triglycerides (TG) were analyzed using specific reagents from BioSino (Beijing, China).

2.5. Histochemical analyses

Small pieces of liver and epididymal adipose tissue were fixed with formalin and embedded in paraffin. Sections (8 μm) were cut and stained with hematoxylin and eosin. Images were captured and analyzed using a CCD Camera (Nikon, Japan)

Table 1
Effect of dietary C3G on animal characteristics in HFD and *db*/*db* mice

Parameter	SFD	HFD	HFD+C3G	*db*/+	*db*/*db*	*db*/*db*+C3G
Initial BW (g)	28.5±0.4	34.0±0.6	34.4±0.6	18.3±0.3	30.2±0.5	30.6±0.6
Final BW (g)	31.0±0.7	40.7±0.8	39.0±0.9	30.0±0.7	48.2±1.0	46.2±0.7
Food intake (g/day)	2.97±0.15	2.75±0.22	2.80±0.25	3.02±0.11	6.76±0.51	6.57±0.62
Tissue weight (% BW)						
Liver	4.01±0.15	4.84±0.22	4.16±0.13 *	4.29±0.11	5.81±0.23	4.66±0.16 #
Heart	0.56±0.04	0.53±0.03	0.49±0.02	0.45±0.02	0.37±0.04	0.36±0.03
Kidneys	1.15±0.04	1.02±0.05	1.08±0.06	1.04±0.02	0.83±0.05	0.79±0.04
Epididymal fat	3.51±0.48	5.36±0.40	5.19±0.42	3.03±0.11	4.73±0.51	4.52±0.44
Subcutaneous fat	0.91±0.03	1.36±0.05	1.40±0.07	0.84±0.02	1.50±0.08	1.51±0.06

Values shown are mean±S.E., n=12. SFD, standard fat diet.
* P<.05 vs HFD.
\# P<.05 vs *db*/*db*.

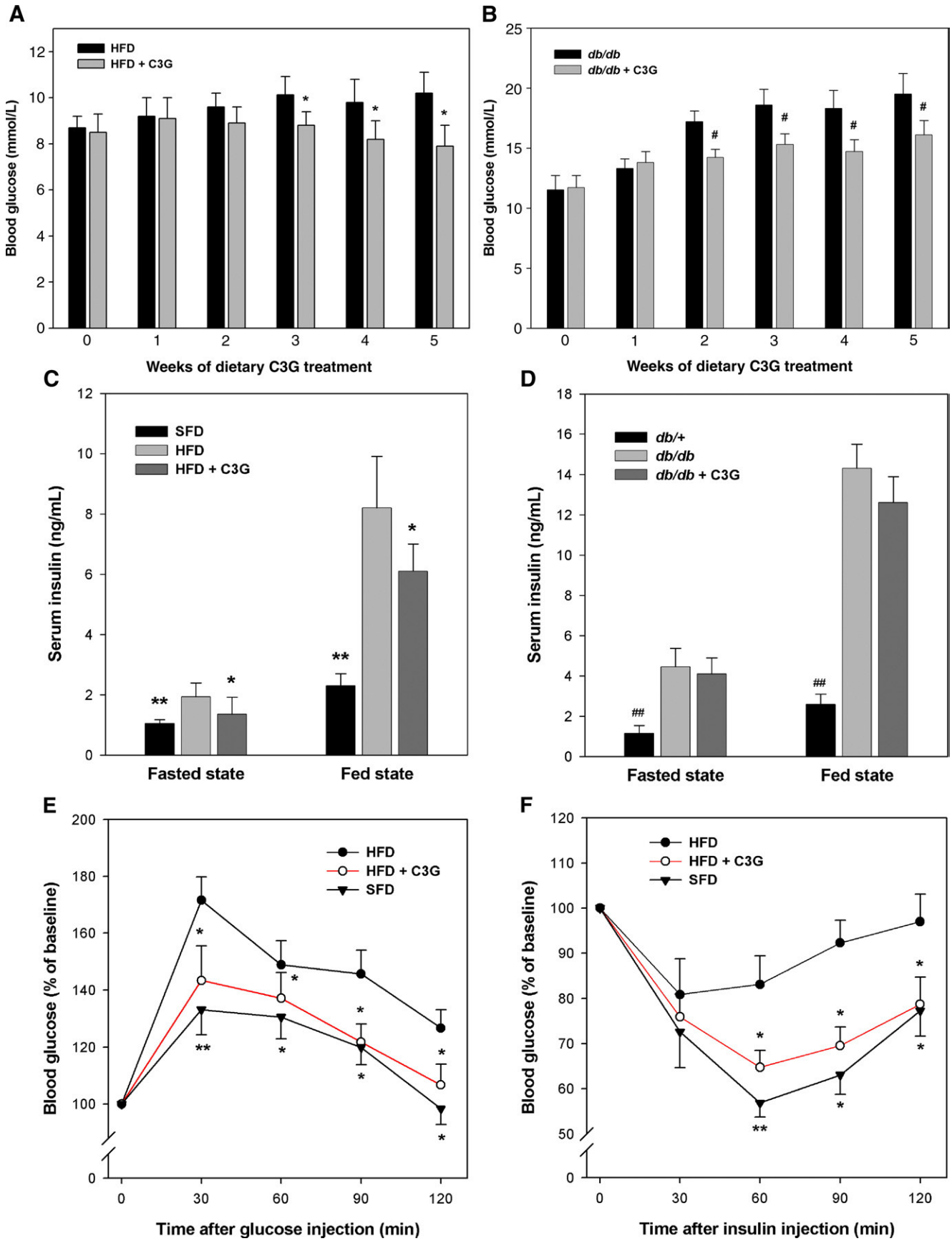

Fig. 1. Effect of dietary C3G on glucose metabolism and insulin sensitivity in HFD and *db*/*db* mice. (A, B) Dietary C3G significantly lowered fasting blood glucose levels in both male HFD (A) and *db*/*db* (B) mice over the course of a 5-week period. (C, D) Serum levels of insulin in mice with the indicated treatments. (E–H) Results of glucose and insulin tolerance tests in HFD (E, F) and *db*/*db* (G, H) mice. Data are shown as the mean±S.E.; n=4–5. *P<.05, **P<.01 versus HFD; $^{\#}P$<.05, $^{\#\#}P$<.01 versus *db*/*db*.

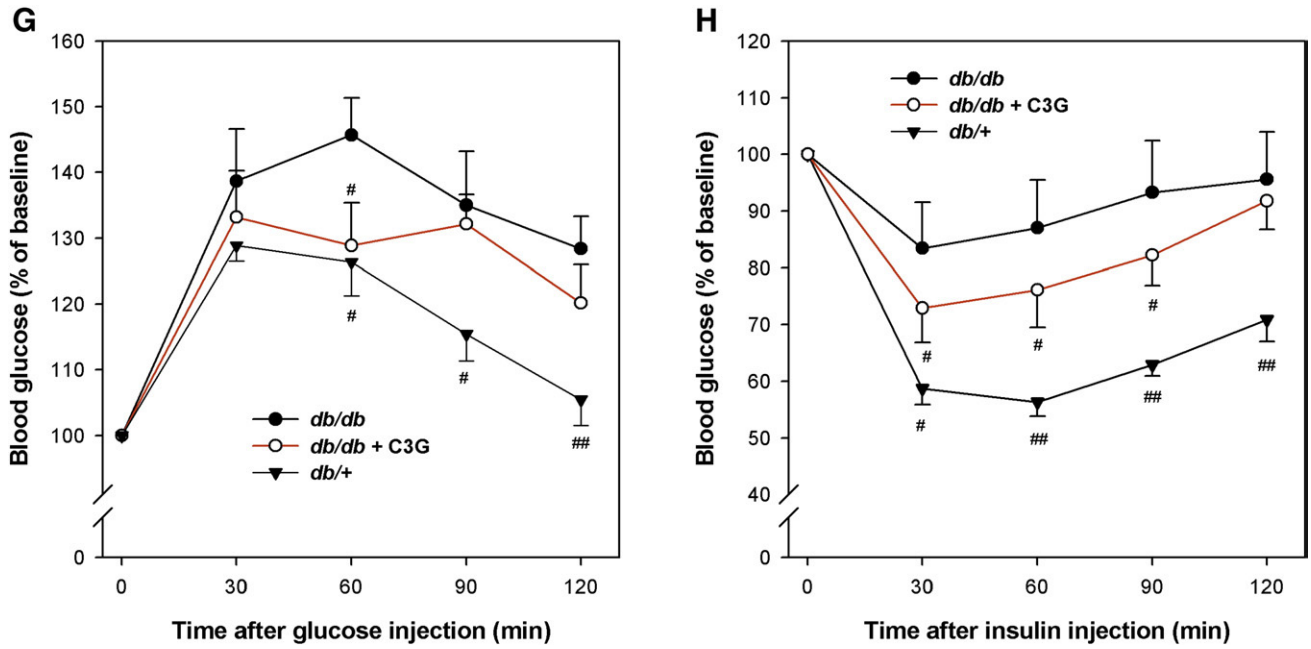

Fig. 1. (*continued*).

at a ×400 magnification. To quantify adipocyte size and the frequency of adipocytes death in individual mice, morphometric data were obtained from digitized tracings of ≥500 adipocytes from three or more sections. The extent of macrophage infiltration into adipose tissue was assessed by the presence of crown-like structures and the messenger RNA (mRNA) expression level of macrophage markers (F4/80 and Cd11c). Steatosis was evaluated in liver specimens using histological steatosis area as described previously [29]. Steatosis area was defined as the surface of empty holes within the tissue (expressed as a percentage), determined by an automated image analyzer (Image-Pro Plus 6.3). The mean surface analyzed per mouse was 2.5 mm^2.

2.6. Quantitative real-time polymerase chain reaction analyses

Total RNA was isolated using Trizol reagent (Invitrogen, Carlsbad, CA, USA). For reverse transcription, 0.5–1.0 μg of the total RNA was converted to the first-strand complementary DNA in 20 μL reactions using a complement DNA synthesis kit (Fermentas, Shenzhen, China). Quantitative real-time polymerase chain reaction (PCR) analyses were performed using SYBR Green MasterMix (GeneCopoeia, Germantown, MD, USA) in a real-time PCR machine (ABI 7500; Applied Biosystem). The thermal cycling program was 3 min at 95°C for enzyme activation and 40 cycles of denaturation for 15 s at 95°C, annealing 30 s at 58°C and extension 30 s at 72°C. Primers used in the present study are listed in supplementary Table S1. To normalize expression data, 18s rRNA was used as an internal control gene. For some experiments, another housekeeping gene, β-actin, was used, and the experiments produced identical results to those obtained when 18s rRNA was used as a reference.

2.7. Protein analysis by Western blotting

Cytoplasmic and nuclear protein extracts from liver and adipose tissues were prepared using NE-PER (Thermo Fisher Scientific, Rockford, IL) extraction reagents (Thermo Scientific, Rockford, IL, USA) according to the manufacturer's instructions. To obtain total protein extracts, the liver and adipose tissues were placed in a cold lysis buffer containing 50 mmol/L Tris-HCl (pH 7.0), 2 mmol/L EGTA, 5 mmol/L EDTA, 30 mmol/L NaF, 10 mmol/L Na_3VO_4, 10 mmol/L $Na_4P_2O_7$, 40 mmol/L β-glycerophosphate, 0.5% NP-40 and 1% protease inhibitor cocktail. After homogenization on ice, the tissue lysates were centrifuged, and the supernatants were used for Western blotting analysis or JNK kinase assay. Protein concentrations were determined by using the bicinchoninic acid protein assay kit from Beyotime (Haimen, China).

Western blotting experiments were performed as described previously [21]. We probed samples with primary antibodies and detected with horseradish peroxidase-conjugated secondary antibodies using ECL detection system (Santa Cruz Biotechnology). The band densities were quantified using an image analyzer Quantity One System (Bio-Rad, Richmond, CA, USA). All protein quantifications were adjusted for the corresponding β-actin level, which was not consistently changed by the different treatment conditions.

2.8. JNK kinase activity assay

The JNK kinase activity was determined using a nonradioactive assay kit (Cell Signaling Technology). Briefly, 200–250 μg of protein/tissue lysate was incubated with N-terminal c-Jun fusion protein bound to glutathione sepharose beads to selectively pull down JNK. The beads were washed three times with kinase buffer, and kinase reaction was carried out in the presence of adenosine triphosphate (ATP) for 30 min at 37°C. The reaction was stopped by adding SDS-sample buffer and boiling the sample. Phosphorylation of c-Jun was measured by Western blotting using a phospho-c-Jun antibody.

2.9. Statistical analyses

Statistical analyses were performed using the SPSS 14.0 package (SPSS Inc., Chicago, IL, USA). All results are expressed as means±S.E. and are analyzed by the Student's *t* test or analysis of variance to determine *P* values; $P<.05$ was considered statistically significant.

3. Results

3.1. Effect of dietary C3G on animal characteristics

Dietary C3G supplementation did not affect the BW gain in both HFD and *db*/*db* mice, accompanied by no significant difference in food intake during the experimental period (Table 1). Heart, kidney, and adipose tissue (subcutaneous and epididymal) weights (% of BW) did not significantly differ between the C3G-treated and their respective nontreated control groups. However, liver weights (% of BW) were significantly lower in the C3G groups than those in the control HFD (4.16±0.13 vs. 4.84±0.22) and *db*/*db* groups (4.66±0.16 vs. 5.81±0.23; all $P<.05$), respectively.

3.2. Effect of dietary C3G on glucose metabolism and insulin sensitivity

We determined that dietary C3G induces significant decreases in blood glucose levels in all groups. After less than 3 weeks of treatment, C3G had already decreased the fasting glucose levels in both HFD and *db*/*db* mice, and this pattern persisted during the subsequent 2 weeks (Fig. 1A, B). Moreover, the serum insulin concentrations in the fasted and refed HFD mice were significantly decreased after 5 weeks of C3G treatment (Fig. 1C), whereas no such decrease was noted in the *db*/*db* mice (Fig. 1D), an effect potentially

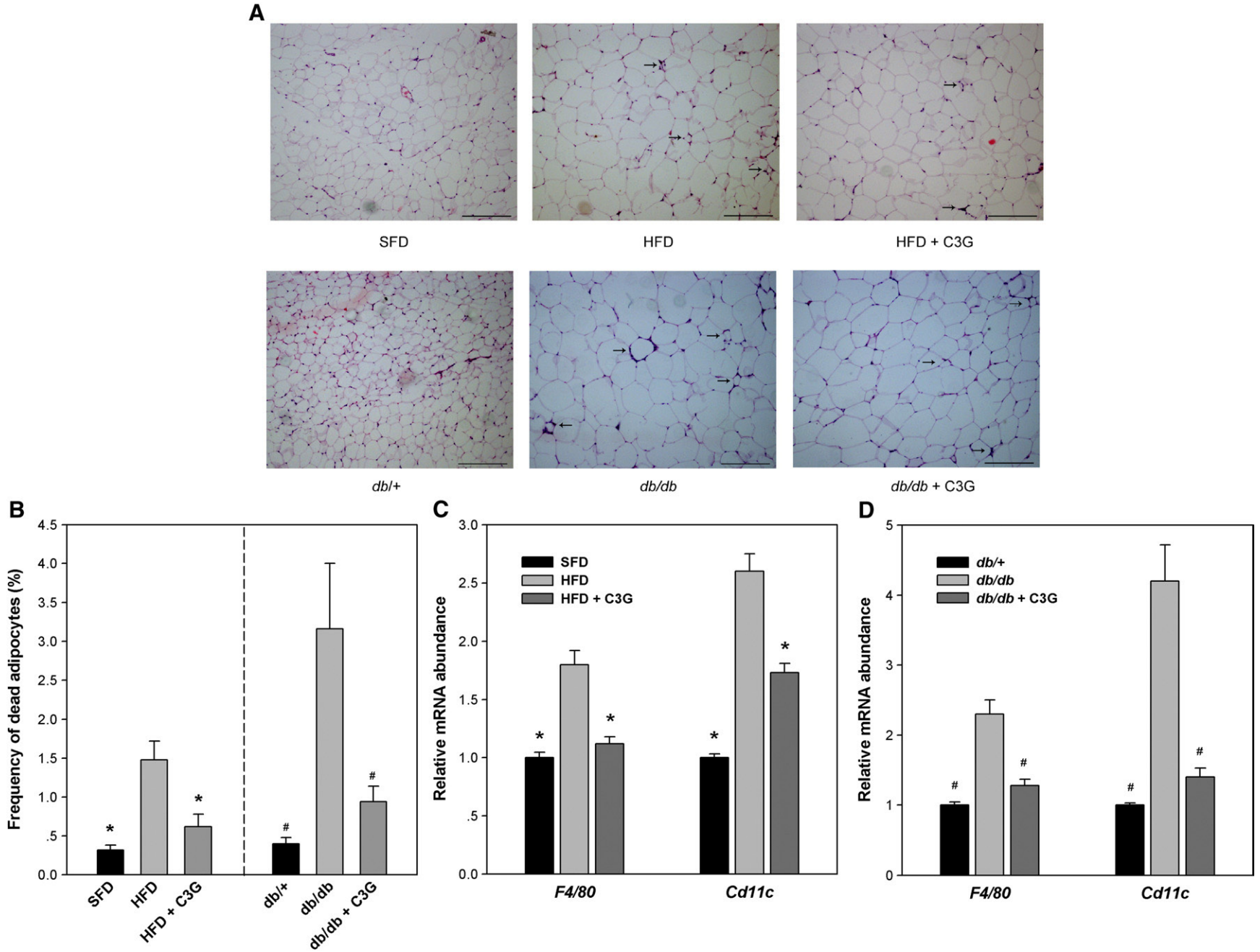

Fig. 2. C3G attenuates the frequency of adipocytes death and macrophage infiltration in adipose tissue of HFD and *db*/*db* mice. (A) Representative hematoxylin and eosin-stained histological sections of adipose tissue from mice are shown. Arrows indicate dead adipocytes surrounded by macrophages. Scale bar=200 μm. (B) Frequency of adipocytes death in mice with the indicated treatments. (C, D) Expression levels of *F4/80* and *Cd11c* genes in adipose tissue of HFD (C) and *db*/*db* (D) mice. Data are shown as the mean±S.E.; n=4–5. *P<.01 versus HFD; #P<.01 vs. *db*/*db*.

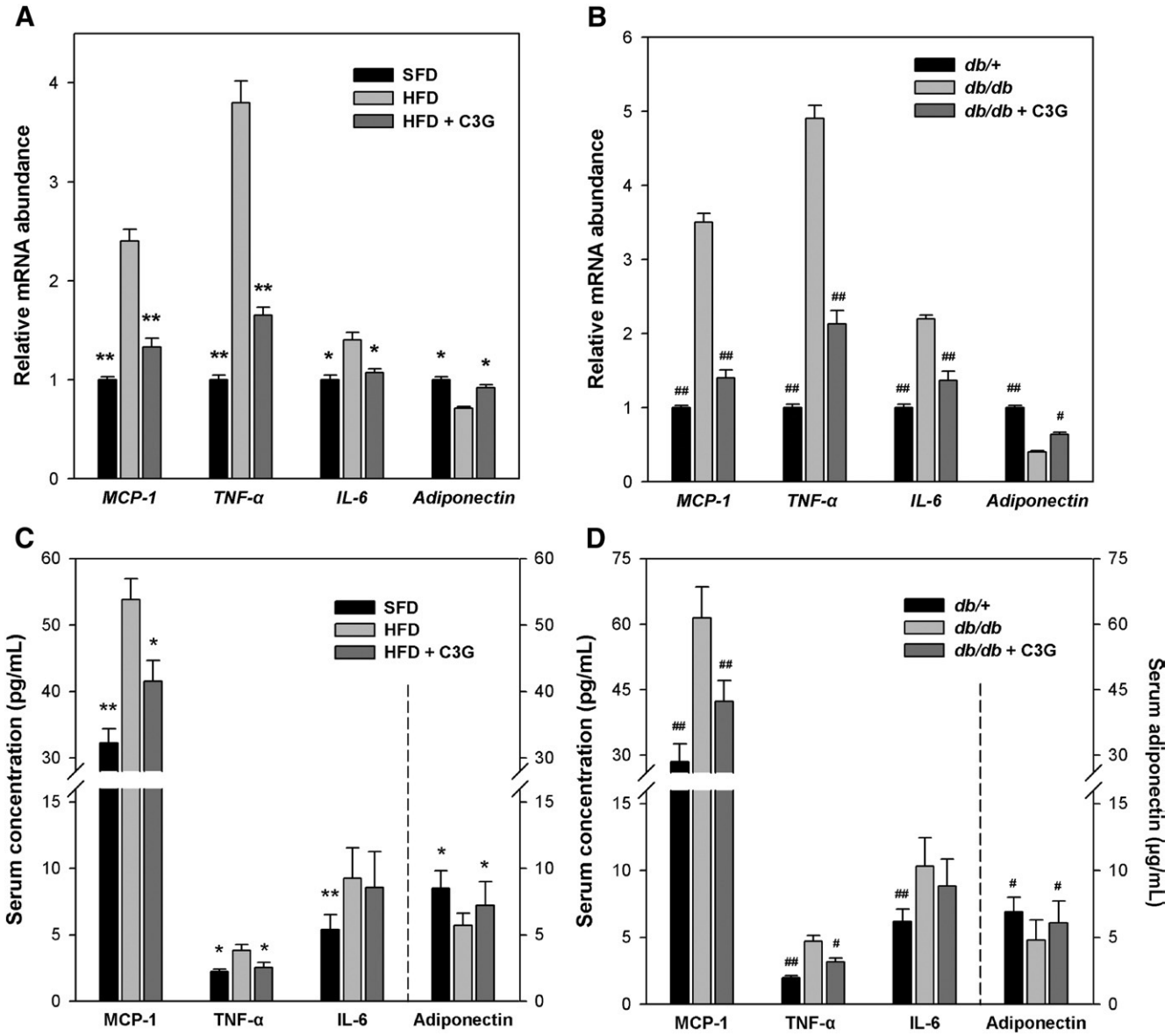

Fig. 3. Gene expression levels in epididymal white adipose tissue (A, B) and serum concentrations of adipocytokines (C, D) in HFD and *db*/*db* mice treated with or without C3G. (A, B) Adipocytokines mRNA expressions were measured by real-time PCR and normalized to the mRNA levels of 18s rRNA or β-actin. (C, D) Serum levels of adipocytokines in HFD (C) and *db*/*db* (D) mice were measured by ELISA. Data are shown as the mean±S.E.; n=4 for (A) and (B); n=6 for (C) and (D); *P<.05, **P<.01 versus HFD; $^{\#}P$<.05, $^{\#\#}P$<.01 versus *db*/*db*.

attributable to the complete absence of leptin receptor in these mice, which has been shown to be associated with severe persistent hyperinsulinemia [30]. Homeostatic model assessment, which is used to quantify insulin resistance, gave scores of 6.9 for HFD, 4.5 for HFD+C3G, 23.1 for *db*/*db* and 16.4 for *db*/*db* +C3G, indicating improved insulin sensitivity after treatment with C3G (HFD vs. HFD+C3G, *db*/*db* vs. *db*/*db* +C3G; P<.05 for each).

To further evaluate the effect of C3G on glucose metabolism and insulin sensitivity, we next conducted intraperitoneal glucose and insulin tolerance tests. HFD feeding impaired glucose tolerance and insulin sensitivity in C57BL/6J mice; however, C3G-treated HFD mice had significantly lower levels of plasma glucose than control HFD mice at 60 min after intraperitoneal glucose or insulin infusion, and the levels tended to remain lower (Fig. 1E, F). Although C3G-treated *db*/*db* mice showed a slight decrease in plasma glucose compared with nontreated *db*/*db* mice only at 60 min after intraperitoneal injection of glucose (Fig. 1G), the plasma glucose concentrations during insulin tolerance test were markedly decreased at 30, 60 and 90 min in C3G-treated *db*/*db* mice (Fig. 1H). Together, these results demonstrated that HFD and *db*/*db* mice treated with C3G for 5 weeks were less insulin resistant and had a mild improvement in glucose homeostasis compared with their respective untreated controls.

3.3. Effect of dietary C3G on obesity-induced macrophage infiltration and inflammation in adipose tissue

Given anthocyanin's antiinflammatory properties in other systems, we investigated the possibility that C3G treatment would improve adipose tissue and systemic manifestations of inflammation in obese diabetic mice. We next examined white adipose tissue from HFD and *db*/*db* mice by histological analysis. Adipocyte size in HFD and *db*/*db* mice treated with or without C3G was comparable (data not shown), but the frequency of adipocytes death and macrophage infiltration in adipose tissue was more severe in HFD and *db*/*db* control mice (Fig. 2A). Supplementation of the diets with C3G was associated with a significant lower frequency (~60% and ~67%,

respectively) of dead adipocytes in both HFD and *db*/*db* mice as compared with untreated animals ($P<.01$; Fig. 2B). In accordance with the results of adipocytes death, two macrophage markers, *F4/80* (*Emr1*) and *Cd11c*, in adipose tissue were markedly reduced in C3G-treated HFD and *db*/*db* mice compared with nontreated controls (Fig. 2C, D), indicating that C3G reduced macrophage infiltration in these obese diabetic mice.

To further evaluate the effect of C3G on adipose inflammation, we next measured the expression and release of inflammation-related adipocytokines by real-time PCR and/or ELISA. As shown in Fig. 3, the mRNA expressions of inflammatory cytokines *Mcp-1*, *Tnf* and *Il-6* in adipose tissue were significantly reduced by C3G compared with those in untreated controls (Fig. 3A, B). Furthermore, serum levels of MCP-1 and TNF-α were lower in HFD and *db*/*db* mice supplemented with dietary C3G than those in the respective controls (Fig. 3C, D). The serum concentrations of IL-6 in the C3G-treated groups tended to be lower than those in the nontreated groups, but not significantly so. On the other hand, the mRNA in adipose tissue and the protein concentrations in serum of adiponectin, an adipocytokine with antidiabetic, antilipogenic and anti-inflammatory properties, were significantly increased in HFD and *db*/*db* mice receiving C3G (Fig. 3A–D). These findings indicate that dietary C3G reduces adipose tissue inflammatory responses by preventing dysregulation of adipocytokines release.

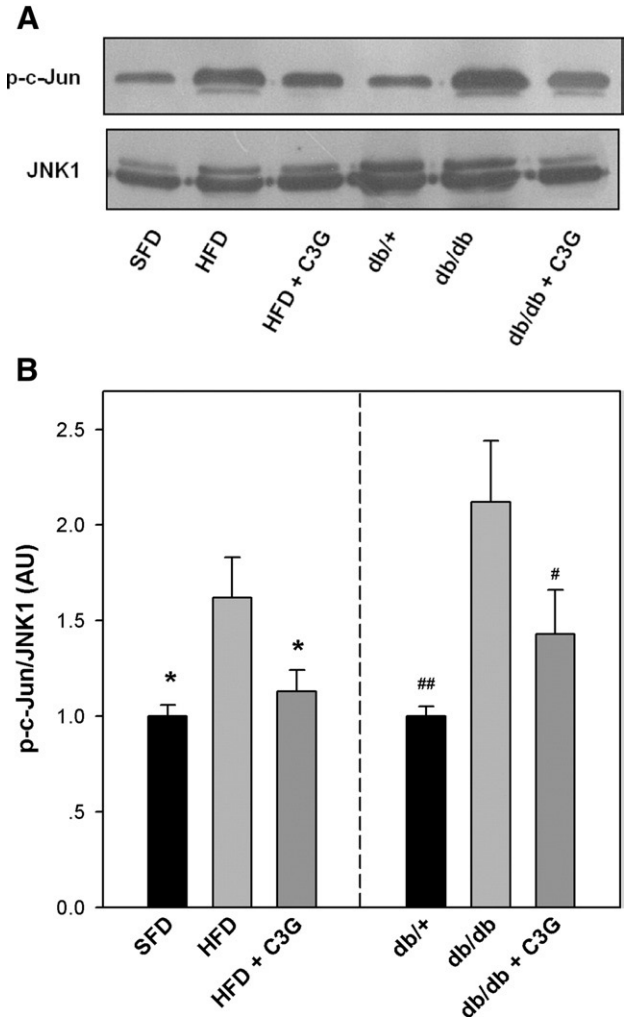

Fig. 4. Effect of dietary C3G on JNK activation in adipose tissue of HFD and *db*/*db* mice. (A) JNK activity was determined by an *in vitro* kinase activity assay using c-Jun as substrate as described in "Materials and Methods." JNK activity was determined by immunoblotting for levels of phosphorylated c-Jun (p-c-Jun). Photographs are representative of three independent experiments each giving similar results. (B) The intensity of bands corresponding to p-c-Jun was corrected by JNK1 protein levels to obtain relative measures of JNK activity between samples. Each bar represents the mean±S.E.; $n=3$. *$P<.05$, versus HFD; #$P<.05$, ##$P<.01$ versus *db*/*db*. AU, arbitrary units.

3.4. Effect of dietary C3G on JNK activation in adipose tissue

Obesity-induced JNK activation is critical in the generation of inflammatory responses and inhibition of insulin action [31,32]. To examine whether C3G modifies the inflammatory profile and insulin action by this mechanism, we determined JNK activity in the adipose tissue of HFD and *db*/*db* mice. Consistent with our previous *in vitro* results [21, 33], we found that C3G treatment resulted in significant inhibition of JNK activation, as indicated by decreases (~29% and ~34%, respectively; $P<.05$ for each) in corrected phospho-c-Jun band density, when compared with untreated control mice (Fig. 4A, B). There were no differences in the JNK1 protein expressions among normal control, C3G-treated and untreated mice.

3.5. Effect of dietary C3G on FoxO1 transcriptional activity in adipose tissue

One mechanism whereby FoxO1 activity is regulated is by nuclear exclusion and subsequent degradation once it is in the cytoplasm [34]. This process is inhibited by JNK activation and promoted by insulin-activated Akt, which phosphorylates FoxO1 at three conserved sites, including Thr-24, Ser-253 and Ser-316 [10]. To verify whether C3G-induced alterations seen in inflammatory mediators and JNK activity in adipose tissue resulted in repression of FoxO1 transcriptional activity, we then prepared whole adipose tissue extracts from mice under the conditions of fasting or refeeding and analyzed the expression and phosphorylation levels of Akt and FoxO1 by Western blotting. Similar to normal control mice, both Ser-473 phosphorylation of Akt and Thr-24 phosphorylation of FoxO1 were significantly increased in the adipose tissue from C3G-treated HFD or *db*/*db* mice after refeeding (Fig. 5A–D). However, refeeding did not alter the phosphorylation levels of Akt and FoxO1 in HFD or *db*/*db* control mice.

Refeeding-induced insulin secretion has been shown to alter FoxO1 subcellular distribution [35]. To further support the above data, we performed Western blotting analysis using cytoplasmic and nuclear fractionations of the adipose tissue extracts. Although the fasting levels of nuclear FoxO1 were relatively low in adipose tissue of C3G-treated HFD and *db*/*db* mice, this could be decreased further by refeeding (Fig. 6A, C). In parallel with this decrease, an increase in cytosolic FoxO1 was observed in these obese diabetic mice treated with C3G. Furthermore, the FoxO1 level in the ratio of nucleus to cytoplasm significantly decreased by C3G (Fig. 6B, D). In contrast, no nuclear decrease or cytosolic increase in FoxO1 level could be detected in untreated HFD and *db*/*db* mice after refeeding. These findings suggest that HFD and *db*/*db* mice are deficient in the nutrient-induced phosphorylation and translocation of FoxO1 in adipose tissue, and this deficiency was improved by C3G.

3.6. Effect of dietary C3G on hepatic steatosis in HFD and db/db mice

Insulin resistance and diabetes can trigger hepatic steatosis, which is associated with inflammation of the liver [1]. We therefore next examined livers in all six groups of mice for morphological alterations, the extent of fatty infiltration and inflammatory responses. Grossly, we found that C3G treatment was associated with significantly lighter and visibly less steatotic livers in the HFD or *db*/*db* mice (Fig. 7A). Examination of hematoxylin and eosin-stained sections demonstrated marked microvesicular steatosis in HFD and *db*/*db* mice, and the

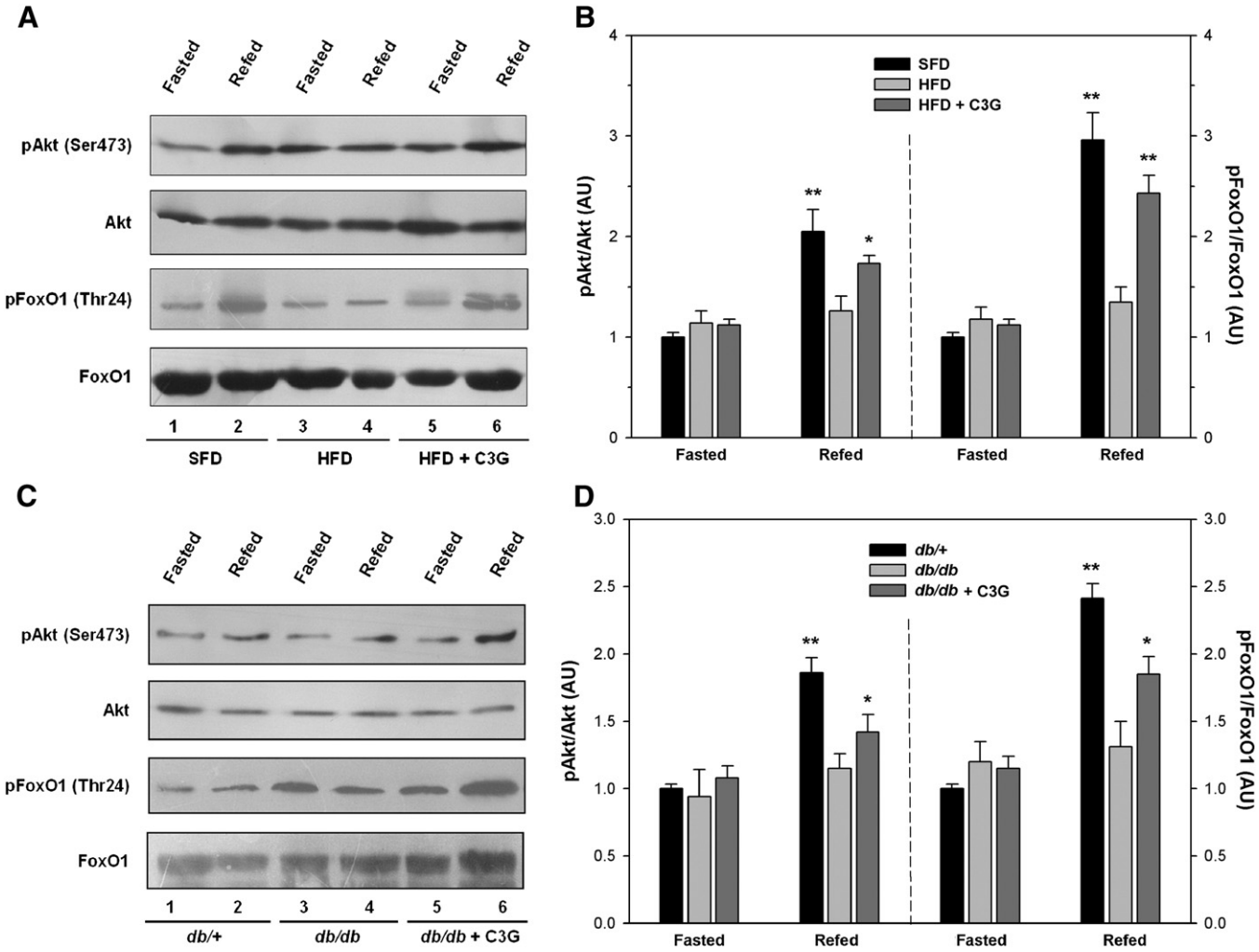

Fig. 5. Effect of dietary C3G on Akt-mediated phosphorylation of FoxO1 in adipose tissue of HFD (A, B) and *db*/*db* (C, D) mice. (A, C) Equal amounts of protein from adipose tissue lysates were immunoblotted by specific antibodies as indicated. Photographs are representative of three independent experiments each giving similar results. (B, D) The intensity of bands corresponding to phospho-Akt (pAkt) and phospho-FoxO1 (pFoxO1) were corrected by respective Akt and FoxO1 protein levels to obtain relative measures of Akt and FoxO1 phosphorylation between samples. Each bar represents the mean±S.E., $n=3$; *$P<.05$, **$P<.01$, compared with fasted mice in the same cohort. AU, arbitrary units.

degree of hepatic steatosis was significantly alleviated by the dietary intake of C3G, as indicated by the reduced surface area of steatosis (Fig. 7B). Consistently, treatment of HFD and *db*/*db* mice with C3G induced significant decreases (by 32±4% and 37±5%, respectively) in hepatic TG contents as compared with control HFD or *db*/*db* mice (Fig. 7C). In agreement with the histological findings, serum alanine aminotransferase levels were substantially reduced in C3G-treated HFD and *db*/*db* mice when compared with nontreated control mice (Fig. 7E). Furthermore, levels of TNF-α mRNAs in the liver were significantly lower in the HFD and *db*/*db* mice supplemented with dietary C3G than those in the respective control mice (Fig. 7D), suggesting that C3G also suppresses the liver tissue inflammation.

3.7. Effect of dietary C3G on FoxO1 localization and its target genes transcription in liver

In a similar way to adipose tissue, C3G treatment markedly decreased the FoxO1 levels in the ratio of nucleus to cytoplasm in the liver tissue of HFD (~45%) and *db*/*db* (~37%) mice after refeeding (Supplementary Fig. S1). We then measured expressions of FoxO1 target genes involved in gluconeogenic and lipogenic pathways. Consistent with previous loss- and gain-of-function experiments [13,36], the augmentation in FoxO1 nuclear exclusion by C3G treatment was associated with diminished expression of key gluconeogenic enzymes in liver (Supplementary Fig. S2), including the glucose-6-phosphatase (*G6Pase*) and phosphoenolpyruvate carboxykinase (*PEPCK*). In addition, the gene expression levels of sterol regulatory element-binding factor 1 and fatty acid synthase were significantly decreased by C3G, suggesting that the attenuation of FoxO1 activity may reduce lipid accumulation by inhibiting TG synthesis.

4. Discussion

This study demonstrated that dietary C3G treatment ameliorates many of the inflammatory consequences of obesity in both HFD and *db*/*db* mice, two widely used animal models of diabesity. Compared with obese diabetic controls, C3G-treated HFD and *db*/*db* mice had decreased macrophage infiltration into adipose tissue, an effect associated with decreased adipose tissue expression of inflammatory molecules. C3G-treated HFD and *db*/*db* mice also had decreased liver TG contents and lighter hepatosteatosis, accompanied by effective attenuation of inflammatory responses in liver. These anti-inflammatory effects of C3G were associated

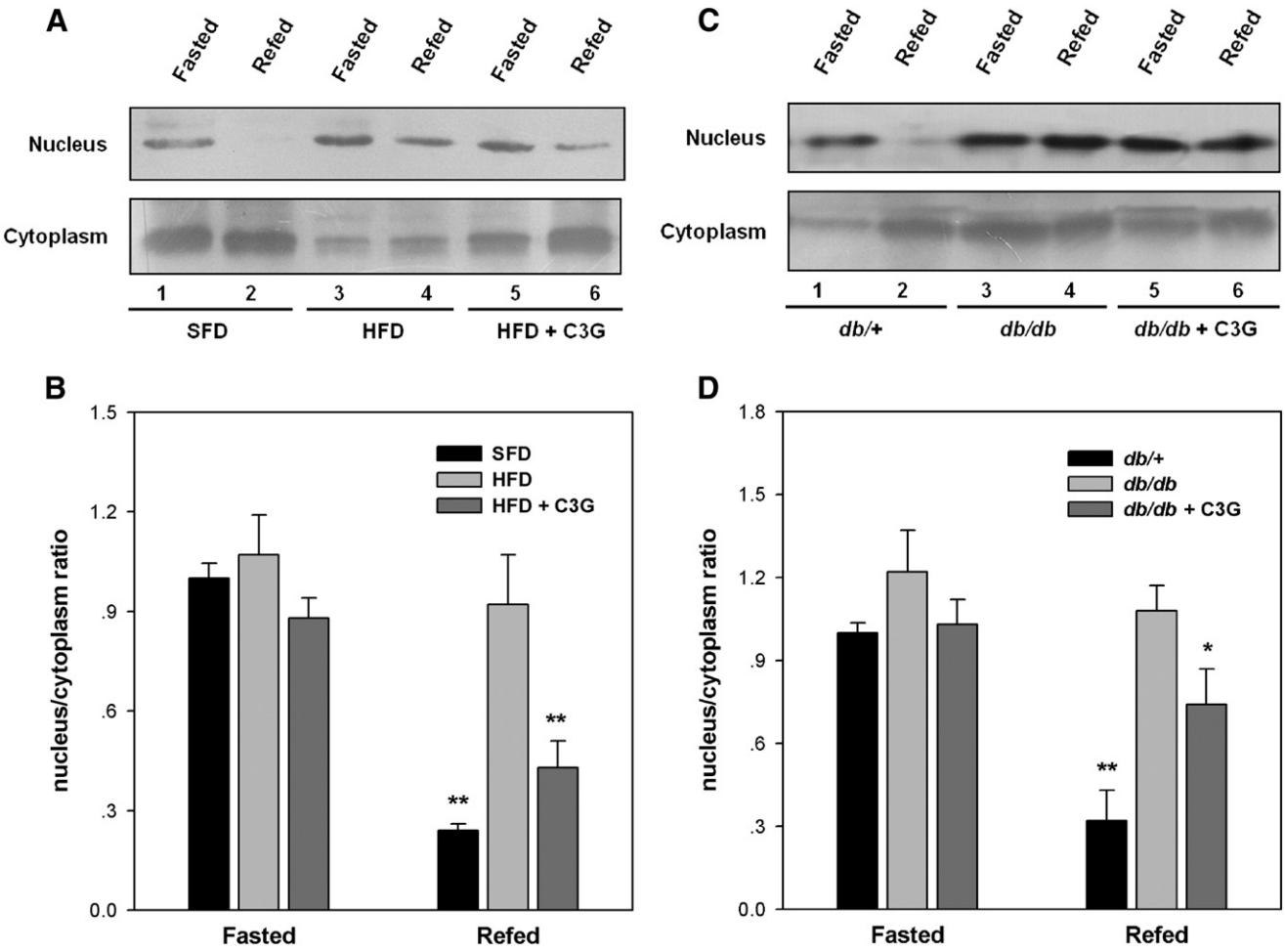

Fig. 6. Effect of dietary C3G on intracellular distribution of FoxO1 in adipose tissue of HFD (A, B) and *db*/*db* (C, D) mice. (A, C) Equal amounts of cytoplasmic and nuclear protein extracts from adipose tissue were immunoblotted by anti-FoxO1 antibody, followed by peroxidase-conjugated appropriate secondary antibody and visualization by ECL detection system. Photographs are representative of three independent experiments each giving similar results. (B, D) The intensity of bands corresponding to FoxO1 in nucleus was corrected by cytoplasmic protein levels to obtain relative measures of FoxO1 transcriptional activity between samples. Each bar represents the mean±S.E.; $n=3$. *$P<.05$, **$P<.01$, compared with fasted mice in the same cohort. AU, arbitrary units.

with improved glucose metabolism and insulin sensitivity in the treated animals as determined by blood glucose levels, glucose and insulin tolerance tests.

Owing to its potent antioxidant and antiinflammatory effects, anthocyanin has been explored as a potential therapeutic modality for a large number of diseases. It suppresses proliferation and induces apoptosis in a wide array of cancer cells [37]. Preclinical studies have shown that dietary anthocyanin-rich extracts ameliorated hyperglycemia and hyperlipidemia by enhancing insulin sensitivity in high-fructose-fed rats and experimental type 2 diabetic mice [23,25,38]. Results from early human trials also have been encouraging. A double-blind, randomized, placebo-controlled trial in humans with dyslipidemia showed that addition of 160 mg anthocyanins twice a day for 12 weeks effectively improved low-density lipoprotein and high-density lipoprotein cholesterol concentrations and enhanced the cellular cholesterol efflux to serum [39]. Given the fact that anthocyanin is poorly absorbed from the gastrointestinal tract and has an excellent safety profile, we chose a high dosage in this study because we wanted to determine early on if oral C3G at any dose could improve diabetes. Based on the average weight and daily food intake (Table 1), the mice would have consumed approximately 160–300 mg C3G per kilogram BW per day. Although such an oral dose would be impractical in humans, the mice were noted to tolerate this dosage quite well without any noticeable detrimental effects on behavior or appetite. The kidneys, liver and heart manifested either an improved or unchanged histopathology.

Several lines of evidence suggest that obesity-related inflammatory components play crucial roles in the development of insulin resistance. Obese adipose tissue secretes a large number of inflammatory cytokines, such as TNF-α, MCP-1 and IL-6, which are known to block insulin signaling in various tissues [1,40,41]. Some reports showed that anthocyanins have a potency of the anti-inflammatory activity [20,42], and down-regulation of TNF-α, MCP-1 and IL-6 can contribute to amelioration of insulin resistance [40,43]. In this study, C3G ingestion significantly reduced macrophage infiltration and the mRNA levels of MCP-1, TNF-α and IL-6 in adipose tissue of HFD and *db*/*db* mice. A significant decrease of serum TNF-α and MCP-1 concentration and increase of adiponectin were also observed in these C3G-treated obese diabetic mice. Accordingly, the insulin-sensitizing effects of C3G in the present study would appear to be mediated by its action on the production of adipocytokines, resulting in suppressing adipose tissue inflammation.

FoxO1 represents a central regulator of metabolism in peripheral tissues [44]. Regulation of the phosphorylation and intracellular localization of FoxO1 is critical to its transcriptional activity. In the fasted status, where FoxO1 is localized to the nucleus, it drives the expression of gluconeogenic enzymes, such as G6Pase and PEPCK [8,13]. In the fed status, insulin markedly increases Akt-mediated

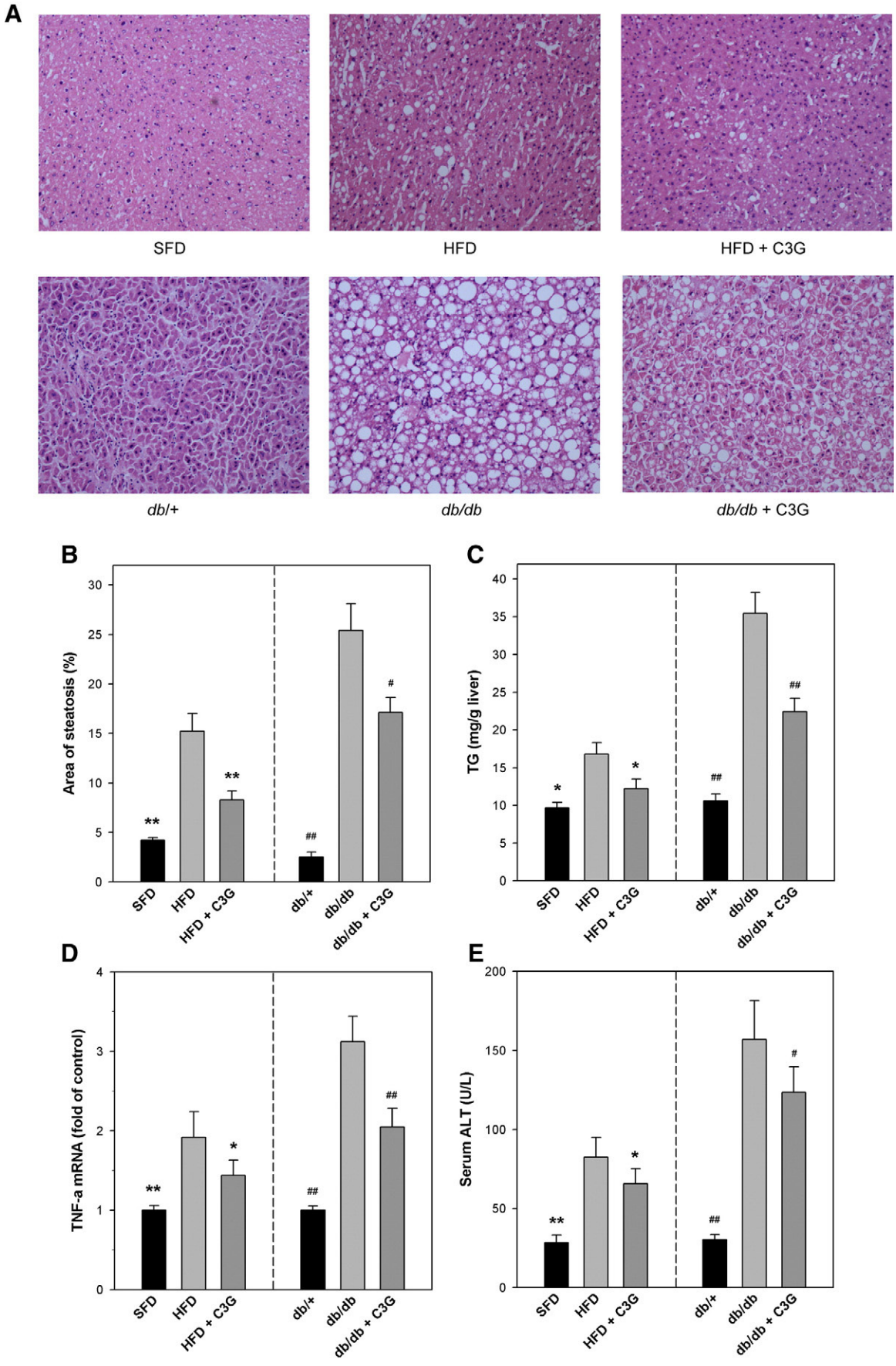
A
SFD
HFD
HFD + C3G
db/+
db/db
db/db + C3G
B
Area of steatosis (%)
C
TG (mg/g liver)
D
TNF-a mRNA (fold of control)
E
Serum ALT (U/L)
SFD
HFD
HFD + C3G
db/+
db/db
db/db + C3G

phosphorylation of FoxO1 and powerfully suppresses gluconeogenesis to protect the body against hyperglycemia [34,44]. Here, we showed that Akt-mediated phosphorylation of FoxO1 by refeeding was impaired in both *db*/*db* and HFD mice, as evidenced by constitutive phosphorylation and nuclear accumulation of FoxO1 throughout each nutritional status. In contrast, dietary C3G enhanced the phosphorylation of Akt and FoxO1 and decreased the FoxO1 levels in the ratio of nucleus to cytoplasm in liver and adipose tissues after refeeding. These changes lead to down-regulation of the G6Pase and PEPCK involving a decrease in the glucose output into the blood and can result in antihyperglycemia. Functional inhibition of FoxO1, caused by hepatic expression of its mutant, has been shown to be associated with reduced hepatic gluconeogenic activity and improved fasting glycemia in diabetic mice [45]. Considering this finding along with our present results, we conclude that the metabolic information on physiological changes due to C3G supplementation is converted into the phosphorylation of FoxO1 via the Akt-dependent pathway, and the extent of phosphorylation represents the FoxO1 transcriptional activity in liver and adipose tissues.

Then, another question arises. How can anthocyanin C3G regulate FoxO1 transcriptional activity in obese or diabetic states? JNK has been shown as a mediator of oxidative stress induced by TNF-α and hyperglycemia and was also revealed to be abnormally activated in obesity and insulin resistance [31,32]. Stress-activated JNK directly increases FoxO1 activity by promoting its import in the nucleus [10]. Notably, a recent study has revealed that H_2O_2 rapidly induced FoxO1 nuclear translocation, but the effect was blocked by JNK inhibitor, suggesting a pivotal role of JNK in FoxO1 activation [11]. Our previous studies have shown that C3G exerts a protective role against H_2O_2- or TNF-α-induced insulin resistance in 3T3-L1 adipocytes by inhibiting the JNK activation [21]. The current study found that dietary C3G reduced the expression levels of TNF-α in the liver and adipose tissues, which was parallel with its inhibition of JNK activation. Based on previous reports and our findings, it is speculated that down-regulation of inflammatory adipocytokines by C3G blocked the overactivation of JNK, and the subsequent modulation of FoxO1 transcriptional activity by C3G may contribute to a decrease in hepatic glucose production and lipid accumulation.

In conclusion, our present study revealed that C3G, which is one of the most typical anthocyanins, reduces blood glucose levels and enhances insulin sensitivity in two mouse models of diabesity. C3G also greatly ameliorated inflammation at the cellular and biochemical levels in white adipose tissue of obese mice. The beneficial effects of C3G against obesity-induced insulin resistance and hepatic steatosis are associated with its inhibition on the JNK/FoxO1 pathway. Further studies are warranted to determine whether anthocyanin may be recommended as an effective strategy for preventing and/or treating diabesity complications in humans.

Supplementary materials related to this article can be found online at doi:10.1016/j.jnutbio.2010.12.013.

References

[1] Nishimura S, Manabe I, Nagai R. Adipose tissue inflammation in obesity and metabolic syndrome. Discov Med 2009;8:55–60.
[2] Zou C, Shao J. Role of adipocytokines in obesity-associated insulin resistance. J Nutr Biochem 2008;19:277–86.
[3] Weisberg SP, McCann D, Desai M, Rosenbaum M, Leibel RL, Ferrante Jr AW. Obesity is associated with macrophage accumulation in adipose tissue. J Clin Invest 2003;112:1796–808.
[4] De Taeye BM, Novitskaya T, McGuinness OP, Gleaves L, Medda M, Covington JW, et al. Macrophage TNF-alpha contributes to insulin resistance and hepatic steatosis in diet-induced obesity. Am J Physiol Endocrinol Metab 2007;293:E713–25.
[5] Alwayn IP, Andersson C, Lee S, Arsenault DA, Bistrian BR, Gura KM, et al. Inhibition of matrix metalloproteinases increases PPAR-alpha and IL-6 and prevents dietary-induced hepatic steatosis and injury in a murine model. Am J Physiol Gastrointest Liver Physiol 2006;291:G1011–9.
[6] Targher G, Bertolini L, Scala L, Poli F, Zenari L, Falezza G. Decreased plasma adiponectin concentrations are closely associated with nonalcoholic hepatic steatosis in obese individuals. Clin Endocrinol (Oxf) 2004;61:700–3.
[7] Nakae J, Biggs III WH, Kitamura T, Cavenee WK, Wright CV, Arden KC, et al. Regulation of insulin action and pancreatic beta-cell function by mutated alleles of the gene encoding forkhead transcription factor Foxo1. Nat Genet 2002;32:245–53.
[8] Matsumoto M, Pocai A, Rossetti L, Depinho RA, Accili D. Impaired regulation of hepatic glucose production in mice lacking the forkhead transcription factor Foxo1 in liver. Cell Metab 2007;6:208–16.
[9] Nakae J, Kitamura T, Kitamura Y, Biggs WH, Arden KC, Accili D. The forkhead transcription factor Foxo1 regulates adipocyte differentiation. Dev Cell 2003;4:119–29.
[10] Essers MA, Weijzen S, de Vries-Smits AM, Saarloos I, de Ruiter ND, Bos JL, et al. FOXO transcription factor activation by oxidative stress mediated by the small GTPase Ral and JNK. EMBO J 2004;23:4802–12.
[11] Shen B, Chao L, Chao J. Pivotal role of JNK-dependent FOXO1 activation in downregulation of kallistatin expression by oxidative stress. Am J Physiol Heart Circ Physiol 2010;298:H1048–54.
[12] Zhao X, Gan L, Pan H, Kan D, Majeski M, Adam SA, et al. Multiple elements regulate nuclear/cytoplasmic shuttling of FOXO1: characterization of phosphorylation- and 14–3–3-dependent and -independent mechanisms. Biochem J 2004;378:839–49.
[13] Matsumoto M, Han S, Kitamura T, Accili D. Dual role of transcription factor FoxO1 in controlling hepatic insulin sensitivity and lipid metabolism. J Clin Invest 2006;116:2464–72.
[14] Nakae J, Cao Y, Oki M, Orba Y, Sawa H, Kiyonari H, et al. Forkhead transcription factor FoxO1 in adipose tissue regulates energy storage and expenditure. Diabetes 2008;57:563–76.
[15] Kim JJ, Li P, Huntley J, Chang JP, Arden KC, Olefsky JM. FoxO1 haploinsufficiency protects against high-fat diet-induced insulin resistance with enhanced peroxisome proliferator-activated receptor gamma activation in adipose tissue. Diabetes 2009;58:1275–82.
[16] Ito Y, Daitoku H, Fukamizu A. Foxo1 increases pro-inflammatory gene expression by inducing C/EBPbeta in TNF-alpha-treated adipocytes. Biochem Biophys Res Commun 2009;378:290–5.
[17] Galvano F, La Fauci L, Lazzarino G, Fogliano V, Ritieni A, Ciappellano S, et al. Cyanidins: metabolism and biological properties. J Nutr Biochem 2004;15:2–11.
[18] He J, Giusti MM. Anthocyanins: natural colorants with health-promoting properties. Annu Rev Food Sci Technol 2010;1:163–87.
[19] Wang Q, Xia M, Liu C, Guo H, Ye Q, Hu Y, et al. Cyanidin-3-*O*-beta-glucoside inhibits iNOS and COX-2 expression by inducing liver × receptor alpha activation in THP-1 macrophages. Life Sci 2008;83:176–84.
[20] Xia M, Ling W, Zhu H, Wang Q, Ma J, Hou M, et al. Anthocyanin prevents CD40-activated proinflammatory signaling in endothelial cells by regulating cholesterol distribution. Arterioscler Thromb Vasc Biol 2007;27:519–24.
[21] Guo H, Ling W, Wang Q, Liu C, Hu Y, Xia M. Cyanidin 3-glucoside protects 3T3-L1 adipocytes against H_2O_2- or TNF-alpha-induced insulin resistance by inhibiting c-Jun NH2-terminal kinase activation. Biochem Pharmacol 2008;75:1393–401.
[22] Tsuda T, Horio F, Uchida K, Aoki H, Osawa T. Dietary cyanidin 3-*O*-beta-D-glucoside-rich purple corn color prevents obesity and ameliorates hyperglycemia in mice. J Nutr 2003;133:2125–30.
[23] Guo H, Ling W, Wang Q, Liu C, Hu Y, Xia M, et al. Effect of anthocyanin-rich extract from black rice (*Oryza sativa* L. *indica*) on hyperlipidemia and insulin resistance in fructose-fed rats. Plant Foods Hum Nutr 2007;62:1–6.
[24] Jayaprakasam B, Olson LK, Schutzki RE, Tai MH, Nair MG. Amelioration of obesity and glucose intolerance in high-fat-fed C57BL/6 mice by anthocyanins and ursolic acid in Cornelian cherry (*Cornus mas*). J Agric Food Chem 2006;54:243–8.
[25] Takikawa M, Inoue S, Horio F, Tsuda T. Dietary anthocyanin-rich bilberry extract ameliorates hyperglycemia and insulin sensitivity via activation of AMP-activated protein kinase in diabetic mice. J Nutr 2010;140:527–33.
[26] Reeves PG, Nielsen FH, Fahey Jr GC. AIN-93 purified diets for laboratory rodents: final report of the American Institute of Nutrition ad hoc writing committee on the reformulation of the AIN-76A rodent diet. J Nutr 1993;123:1939–51.
[27] Levy JC, Matthews DR, Hermans MP. Correct homeostasis model assessment (HOMA) evaluation uses the computer program. Diabetes Care 1998;21:2191–2.
[28] Folch J, Lees M, Sloane Stanley GH. A simple method for the isolation and purification of total lipides from animal tissues. J Biol Chem 1957;226:497–509.
[29] Alessi MC, Bastelica D, Mavri A, Morange P, Berthet B, Grino M, et al. Plasma PAI-1 levels are more strongly related to liver steatosis than to adipose tissue accumulation. Arterioscler Thromb Vasc Biol 2003;23:1262–8.
[30] Kobayashi K, Forte TM, Taniguchi S, Ishida BY, Oka K, Chan L. The db/db mouse, a model for diabetic dyslipidemia: molecular characterization and effects of Western diet feeding. Metabolism 2000;49:22–31.

Fig. 7. Effect of dietary C3G on liver steatosis and inflammatory responses in HFD and *db*/*db* mice. (A) Representative hematoxylin and eosin-stained histological sections of liver from mice are shown. Original magnification, ×400. (B–E) C3G alleviates obesity-induced hepatic steatosis and inflammatory responses as assessed by decreased steatosis area (B), TG contents (C) and TNF-α mRNA expression (D) in the liver and reduced alanine aminotransferase (ALT) levels in serum (E). Data are shown as the mean±S.E.; n=4–5. *P<.05, **P<.01 versus HFD; $^{\#}P$<.05, $^{\#\#}P$<.01 versus *db*/*db*.

[31] Nguyen MT, Satoh H, Favelyukis S, Babendure JL, Imamura T, Sbodio JI, et al. JNK and tumor necrosis factor-alpha mediate free fatty acid-induced insulin resistance in 3T3-L1 adipocytes. J Biol Chem 2005;280:35361–71.
[32] Hirosumi J, Tuncman G, Chang L, Gorgun CZ, Uysal KT, Maeda K, et al. A central role for JNK in obesity and insulin resistance. Nature 2002;420:333–6.
[33] Xia M, Ling W, Zhu H, Ma J, Wang Q, Hou M, et al. Anthocyanin attenuates CD40-mediated endothelial cell activation and apoptosis by inhibiting CD40-induced MAPK activation. Atherosclerosis 2009;202:41–7.
[34] Matsuzaki H, Daitoku H, Hatta M, Tanaka K, Fukamizu A. Insulin-induced phosphorylation of FKHR (Foxo1) targets to proteasomal degradation. Proc Natl Acad Sci U S A 2003;100:11285–90.
[35] Aoyama H, Daitoku H, Fukamizu A. Nutrient control of phosphorylation and translocation of Foxo1 in C57BL/6 and db/db mice. Int J Mol Med 2006;18:433–9.
[36] Zhang W, Patil S, Chauhan B, Guo S, Powell DR, Le J, et al. FoxO1 regulates multiple metabolic pathways in the liver: effects on gluconeogenic, glycolytic, and lipogenic gene expression. J Biol Chem 2006;281:10105–17.
[37] Wang LS, Stoner GD. Anthocyanins and their role in cancer prevention. Cancer Lett 2008;269:281–90.
[38] Sasaki R, Nishimura N, Hoshino H, Isa Y, Kadowaki M, Ichi T, et al. Cyanidin 3-glucoside ameliorates hyperglycemia and insulin sensitivity due to down-regulation of retinol binding protein 4 expression in diabetic mice. Biochem Pharmacol 2007;74:1619–27.
[39] Qin Y, Xia M, Ma J, Hao Y, Liu J, Mou H, et al. Anthocyanin supplementation improves serum LDL- and HDL-cholesterol concentrations associated with the inhibition of cholesteryl ester transfer protein in dyslipidemic subjects. Am J Clin Nutr 2009;90:485–92.
[40] Kanda H, Tateya S, Tamori Y, Kotani K, Hiasa K, Kitazawa R, et al. MCP-1 contributes to macrophage infiltration into adipose tissue, insulin resistance, and hepatic steatosis in obesity. J Clin Invest 2006;116:1494–505.
[41] de Alvaro C, Teruel T, Hernandez R, Lorenzo M. Tumor necrosis factor alpha produces insulin resistance in skeletal muscle by activation of inhibitor kappaB kinase in a p38 MAPK-dependent manner. J Biol Chem 2004;279:17070–8.
[42] Seymour EM, Lewis SK, Urcuyo-Llanes DE, Tanone II, Kirakosyan A, Kaufman PB, et al. Regular tart cherry intake alters abdominal adiposity, adipose gene transcription, and inflammation in obesity-prone rats fed a high fat diet. J Med Food 2009;12:935–42.
[43] Lumeng CN, Deyoung SM, Saltiel AR. Macrophages block insulin action in adipocytes by altering expression of signaling and glucose transport proteins. Am J Physiol Endocrinol Metab 2007;292:E166–74.
[44] Gross DN, Wan M, Birnbaum MJ. The role of FOXO in the regulation of metabolism. Curr Diab Rep 2009;9:208–14.
[45] Altomonte J, Richter A, Harbaran S, Suriawinata J, Nakae J, Thung SN, et al. Inhibition of Foxo1 function is associated with improved fasting glycemia in diabetic mice. Am J Physiol Endocrinol Metab 2003;285:E718–28.